RIMS Kôkyûroku Bessatsu
B15 (2009), 125–146

Conservative numerical schemes for the Keller-Segel system and numerical results

Dedicated to Professor Toshitaka Nagai on the occasion of his sixtieth birthday

By

Norikazu SAITO*

Abstract

We summarize conservative numerical schemes for the Keller-Segel system modelling chemotaxis. The advantage of our schemes is that they satisfy the conservation of positivity and total mass. Both finite-difference and finite-element methods are considered. We also report some numerical results, which will be of use in analysis of the Keller-Segel system.

§ 1. Introduction

This paper is concerned with conservative numerical schemes to the Keller-Segel system of chemotaxis (cf. Keller and Segel [8]),

$$u_t - \nabla \cdot (\nabla u - u\nabla v) = 0 \quad \text{and} \quad kv_t - \Delta v + v - u = 0,$$

where, as usual, u denotes the density of the cellular slime molds, v the concentration of the chemical substance, and $k \geq 0$ the relaxation time. We consider the system in a bounded domain Ω with the zero flux boundary condition. The solution $u = u(x,t)$, $(x,t) \in \overline{\Omega} \times [0,T]$, satisfies the conservation of the L^1 norm:

$$\|u(t)\|_{L^1(\Omega)} = \|u(0)\|_{L^1(\Omega)},$$

Recieved March 1, 2009. Revised June 17, 2009. Accepted June 29, 2009.
2000 Mathematics Subject Classification(s): 65M60, 65M06, 35K55
Key Words: finite-element method, finite-difference method, Keller-Segel system
Supported by Grants-in-Aid for Scientific Research (No. 18740046), JSPS, Japan, and by Global COE Program (The Research and Training Center for New Development in Mathematics, The University of Tokyo), MEXT, Japan.
*Graduate School of Mathematical Sciences, The University of Tokyo, Tokyo 153-8914 Japan
e-mail: norikazu@ms.u-tokyo.ac.jp

which is a readily consequence of the conservation of positivity

$$u(x,0) \geq 0, \not\equiv 0 \text{ on } \Omega \quad \Rightarrow \quad u(x,t) > 0 \text{ in } \Omega \times (0,T]$$

and the conservation of total mass

$$\int_\Omega u(x,t)\ dx = \int_\Omega u(x,0)\ dx \qquad (t \in [0,T]).$$

Indeed, those conservation properties play an important role to study the Keller-Segel system; See, for example, Horstmann [6], [7], and Suzuki [16]. Thus, those properties are essential requirements, and it is desirable that numerical solutions preserve them, when we solve the Keller-Segel system by numerical methods. In the present paper, by a *conservative numerical scheme*, we mean a numerical scheme that satisfies the discrete analogue of those analytical properties. Whereas those conservation properties are simple to hold in a continuous problem, some difficulties arise in a discrete problem. To illustrate those difficulties, we consider a linear convection-diffusion equation for the function $u = u(x,t)$ defined on $[0,1] \times [0,\infty)$,

(1.1) $$u_t = [u_x - b(x,t)u]_x\,,$$

where $b(x,t) \geq 0$ denotes a given function. We assume that $u(x,t)$ and $b(x,t)$ are periodic in $x \in [0,1]$ for all $t \geq 0$. The standard explicit finite-difference approximation to (1.1) is given as

$$\frac{u_i^{n+1} - u_i^n}{\tau} = \frac{u_{i-1}^n - 2u_i^n + u_{i+1}^n}{h^2} - \frac{b_{i+1}^n u_{i+1}^n - b_{i-1}^n u_{i-1}^n}{2h}$$

for $1 \leq i \leq N$ and $n \geq 0$, where $u_i^n \approx u(ih, n\tau)$, $b_i^n = b(ih, n\tau)$, $h = 1/N$ and $\tau > 0$. As readily see, if

(1.2) $$\tau \leq \frac{1}{2}h^2, \quad h \leq \frac{2}{\beta^n} \quad \left(\beta^n = \max_{x\in[0,1]} b(x, n\tau)\right),$$

then we have the conservation of non-negativity

(1.3) $$u_i^n \geq 0\ (1 \leq i \leq N) \quad \Rightarrow \quad u_i^{n+1} \geq 0\ (1 \leq i \leq N).$$

(It should be noticed that the conservation of positivity cannot be expected to hold, since we consider the explicit scheme.) However, if we apply this method to the Keller-Segel system, the coefficient function $b(x,t)$ corresponds to $\nabla v (= v_x)$. Thus, we cannot guarantee that (1.2) holds before computations, since we do not know a priori bound for v_x. We meet the same issue, if dealing with the implicit scheme. This means that the conservation of positivity/non-negativity is not simple to hold in a discrete level.

To overcome this issue, it is known that the upwind type approximation is of use. For example, a simple upwind finite-difference approximation to (1.1) is given as

$$\frac{u_i^{n+1} - u_i^n}{\tau} = \frac{u_{i-1}^n - 2u_i^n + u_{i+1}^n}{h^2} - \frac{b_i^n u_i^n - b_{i-1}^n u_{i-1}^n}{h}.$$

In this scheme, (1.3) is satisfied, if

$$\tau \leq \frac{h^2}{2 + h\beta^n}. \tag{1.4}$$

Therefore, in order to guarantee (1.3), we take a variable time increment τ_n subject to (1.4) instead of the fixed time increment τ. In §2, we shall consider a simplified Keller-Segel system ($k = 0$) in a unit circle and state a conservative finite-difference scheme based on this idea. This conservative scheme is essentially the same as the one described in our previous paper, Saito and Suzuki [15], where we treat the zero flux boundary condition. Such a strategy could be extended to the finite-element method. Thus we can deal with multidimensional cases and arbitrary shapes of domains. In §4, we shall review conservative finite-element schemes proposed by Saito [13] and [14]. As a matter of fact, application of the upwind technique to the finite-element method usually destroys the conservation of total mass. To surmount this obstacle, we combine our strategy for the finite-difference method with Baba-Tabata's upwind finite-element method that is proposed by Baba and Tabata [2]. Moreover, for finite-element schemes, we could obtain convergence theorems with explicit convergence rates that will be also recalled in §4. At this stage, we point out that the conservation of total mass is satisfied by the standard finite-element method and this can be verified by taking the unity as the test function. The important point, however, is that our finite-element schemes satisfy both the positivity and mass conservation properties *simultaneously*.

The main contribution of this paper is described in §3 and §5. There, we shall reports some numerical results obtained by our conservative numerical schemes and see that numerical solutions remain bounded if the initial values are sufficiently small.

Before concluding this Introduction, we briefly discuss some other results that are related to numerical methods for the Keller-Segel system. Nakaguchi and Yagi [11] presented finite-element/Runge-Kutta discretizations for the Keller-Segel system without any numerical results. They also established error estimates in the $H^{1+\varepsilon}$ norm, $\varepsilon \in (0, 1/2)$, for a sufficiently small T, though they devoted little attention to conservation of the L^1 norm of approximate solutions. Marrocco [10] discussed mixed finite-element approximations for the simplified Keller-Segel system and offered various numerical examples, but a convergence analysis was not undertaken. The aim of Filbet [3] is similar as ours. He proposed a finite-volume method for the simplified Keller-Segel system, and his approximation of the "chemotaxis term" is essentially the same as ours.

He also derived the L^1 conservation under some condition on the time increment and proved the convergence of the finite-volume solution if the L^1 norm of an initial datum is sufficiently small. On the contrary, we shall pose no assumption on the size of an initial datum and obtain explicit error estimates.

§ 2. Conservative finite-difference method

In order to illustrate the idea of discretization, we consider the finite-difference method to a simplified Keller-Segel system defined in $\mathbb{R}/(2\pi\mathbb{Z}) \times [0,\infty)$,

$$\begin{cases} u_t - [u_x - (\phi(v))_x u]_x = 0, & (x,t) \in \mathbb{R}/(2\pi\mathbb{Z}) \times (0,\infty), \\ -v_{xx} + v = u, & (x,t) \in \mathbb{R}/(2\pi\mathbb{Z}) \times (0,\infty), \\ u|_{t=0} = u_0(x), & x \in \mathbb{R}/(2\pi\mathbb{Z}), \end{cases} \tag{2.1}$$

where $\phi : [0,\infty) \to \mathbb{R}$ and $u_0 \geq 0, \not\equiv 0$ are given functions. Take a positive integer N and set $h = 2\pi/N$. We introduce two kinds of grid points over $[0, 2\pi]$ as

$$x_i = \left(i - \frac{1}{2}\right) h \qquad (i = 1, \ldots, N), \qquad \hat{x}_i = ih \qquad (i = 0, \ldots, N).$$

Grid points over $[0,\infty)$ are defined by

$$t_n = \tau_1 + \cdots + \tau_n \qquad (n = 1, 2, \ldots),$$

where the time increment $\tau_n > 0$ will be determined later. Then, we shall find

$$u_i^n \approx u(x_i, t_n) \quad \text{and} \quad v_i^n \approx v(\hat{x}_i, t_n).$$

Set

$$\mathbf{u}^n = (u_1^n, \ldots, u_N^n)^{\mathrm{T}} \quad \text{and} \quad \mathbf{v}^n = (v_0^n, \ldots, v_N^n)^{\mathrm{T}}.$$

For the time being, we suppose that $\mathbf{u}^{n-1}$ and $\mathbf{v}^{n-1}$ have been obtained and describe schemes for solving $\mathbf{u}^n$ and $\mathbf{v}^n$ separately.

Scheme for solving $\mathbf{u}^n$ The key point is to introduce a *reasonable* approximation of the flux $F = -u_x + (\phi(v))_x u$ of u by applying upwind technique. We set

$$b_i^n = \frac{\phi(v_i^n) - \phi(v_{i-1}^n)}{h} \quad (1 \leq i \leq N), \qquad \mathbf{b}^n = (b_1^n, \ldots, b_N^n)^{\mathrm{T}}. \tag{2.2}$$

Further, we set

$$b_i^{n,+} = \max\{0, b_i^n\} \quad \text{and} \quad b_i^{n,-} = \max\{0, -b_i^n\}.$$

Obviously, b_i^n is an approximation of $(\phi(v))_x$ at $x = x_i$. We note that F is expressed as $F = -u_x + [b]_+ u - [b]_- u$, where $b = (\phi(v))_x$ and $[b]_\pm = \max\{0, \pm b\}$. Hence, following a technique of upwind approximation, we may suppose that u_i^n and u_{i+1}^n are carried into a point $\hat{x}_i$ on flows $b_i^{n,+}$ and $-b_{i+1}^{n,-}$, respectively. That is, a discrete flux F_i^n of $\mathbf{u}^n$ at $x = \hat{x}_i$ is given by

$$F_i^n = -\frac{u_{i+1}^n - u_i^n}{h} + b_i^{n,+} u_i^n - b_{i+1}^{n,-} u_{i+1}^n \quad (i = 0, \dots, N),$$

where we have defined as

$$u_0^n = u_N^n, \quad u_{N+1}^n = u_1^n, \quad b_0^n = b_N^n, \quad b_{N+1}^n = b_1^n.$$

Then our proposed scheme is

$$\frac{u_i^{n+1} - u_i^n}{\tau_{n+1}} = -\frac{F_i^n - F_{i-1}^n}{h} \qquad (i = 1, \dots, N), \tag{2.3}$$

or, equivalently,

$$\begin{aligned} u_i^{n+1} = {} & \lambda_{n+1}(1 + h b_{i-1}^{n,+}) u_{i-1}^n + \left[1 - \lambda_{n+1}(2 + h(b_i^{n,+} + b_i^{n,-}))\right] u_i^n \\ & + \lambda_{n+1}(1 + h b_{i+1}^{n,-}) u_{i+1}^n, \qquad (i = 1, \dots, N), \end{aligned} \tag{2.4}$$

where $\lambda_{n+1} = \tau_{n+1}/h^2$.

We introduce

$$\|\mathbf{b}\|_\infty = \max_{1 \le i \le N} |b_i| \qquad (\mathbf{b} = (b_1, \dots, b_N)^{\mathrm{T}} \in \mathbb{R}^N).$$

By Eqn (2.4), we have

$$\tau_{n+1} \le \frac{h^2}{2 + h\|\mathbf{b}^n\|_\infty} \qquad \Rightarrow \qquad u_i^{n+1} \ge 0 \quad (1 \le i \le N).$$

On the other hand, Eqn (2.3) implies

$$\sum_{i=1}^N u_i^{n+1} = \sum_{i=1}^N u_i^n.$$

Therefore, if taking

$$\tau_{n+1} = \min\left\{\tau, \ \frac{\varepsilon h^2}{2 + h\|\mathbf{b}^n\|_\infty}\right\} \tag{2.5}$$

with $\tau > 0$ and $\varepsilon \in (0, 1]$, we have

$$\|\mathbf{u}^n\|_{1,h} = \|\mathbf{u}^0\|_{1,h},$$

where $\|\cdot\|_{1,h}$ is the discrete L^1 norm defined as

$$\|\mathbf{u}\|_{1,h} = \sum_{i=1}^N |u_i| h \qquad (\mathbf{u} = (u_1, \dots, u_N)^{\mathrm{T}} \in \mathbb{R}^N).$$

Scheme for solving $\mathbf{v}^n$. We describe two methods. The first one is the finite-difference method. That is, $\mathbf{v}^n$ is computed by

$$\begin{cases} -\dfrac{v_{i-1}^n - 2v_i^n + v_{i+1}^n}{h^2} + v_i^n = \hat{u}_i^n & (0 \le i \le N) \\ v_0^n = v_N^n, \quad v_{-1}^n = v_{N-1}^n, \quad v_1^n = v_{N+1}^n & (n \ge 0), \end{cases}$$

where $\hat{u}_i^n = (u_{i+1}^n + u_i^n)/2$. This implies a linear system for $\mathbf{v}^n$, however the coefficient matrix is not tri-diagonal.

The second method makes use of the discrete Fourier series. Thus, if $\mathbf{u}^n$ is expressed by the discrete Fourier series as

$$\hat{u}_i^n = \frac{1}{2}a_0 + \sum_{k=1}^{N/2-1} (a_k \cos k\hat{x}_i + b_k \sin k\hat{x}_i) + \frac{1}{2}a_{N/2} \cos\big((N/2)\hat{x}_{N/2}\big),$$

$$a_k = \frac{2}{N}\sum_{j=0}^{N-1} \hat{u}_j^n \cos(k\hat{x}_j), \qquad b_k = \frac{2}{N}\sum_{j=1}^{N-1} \hat{u}_j^n \sin(k\hat{x}_j),$$

then $\mathbf{v}^n$ is obtained by

$$v_i^n = \frac{a_0}{2} + \sum_{k=1}^{N/2-1} \frac{1}{1+k^2}(a_k \cos k\hat{x}_i + b_k \sin k\hat{x}_i) + \frac{1}{2}\cdot\frac{a_{N/2}}{1+N^2/4}\cos\big((N/2)\hat{x}_{N/2}\big),$$

where N is assumed to be even. The Fourier coefficients $\{a_k\}$ and $\{b_k\}$ are computed by FFT (e.g. Ooura [12] etc.) readily and efficiently.

Remark. In this section, we have considered only the explicit time discreization. However, the implicit time discretizations are also available. In fact, in [15], we proposed the conservative finite difference/implicit-θ-scheme for a simplified Keller-Segel system in an interval $[0, 1]$ under the zero-flux boundary condition

$$u_x - (\phi(v))_x u = 0, \quad v_x = 0 \qquad (x = 0, 1),$$

and proved the conservation of the L^1 norm. An application of our conservative scheme to tumor angiogenesis model is reported in Kubo et al. [9].

§ 3. Numerical results (1D case)

We follow the notation of the previous section and continue to consider (2.1). Throughout this section, we suppose $\phi(v) = \lambda v$ with a constant $\lambda > 0$. Then, as is well-known, (2.1) admits a unique classical solution which is global in time. We are interested in whether the solution converges to a non-trivial stationary solution. Below, we report some results of numerical experiments by using the finite-difference scheme (2.3) with the time increment control (2.5).

With a positive parameter α, we take the following four initial functions:

$$u_0(x) = \left(\alpha - \frac{2\pi}{10}\right) w_i(x) + \frac{1}{10} \qquad (i = 1, 2, 3), \tag{3.1}$$

$$u_0(x) = \frac{\alpha}{2\pi^2} \min\{x,\ 2\pi - x\}(2 + \sin(3x)), \tag{3.2}$$

where

$$w_1(x) = \begin{cases} 1/(2\kappa) & (7\kappa \le x \le 9\kappa) \\ 0 & (\text{otherwise}) \end{cases} \qquad (\kappa = 2\pi/16),$$

$$w_2(x) = \begin{cases} 1/(4\kappa) & (\kappa \le x \le 3\kappa,\ 5\kappa \le x \le 7\kappa) \\ 0 & (\text{otherwise}) \end{cases} \qquad (\kappa = 2\pi/8),$$

$$w_3(x) = \begin{cases} 1/(4\kappa) & (\kappa \le x \le 3\kappa,\ 4\kappa \le x \le 6\kappa) \\ 0 & (\text{otherwise}) \end{cases} \qquad (\kappa = 2\pi/8).$$

Then, we have $\alpha = \|\mathbf{u}^0\|_{1,h}$ and thus $\alpha = \|\mathbf{u}^n\|_{1,h}$ for $n \ge 1$.

Results are displayed in Fig. 1–4 where $\lambda = 5$, $h = 2\pi/256$, $\tau = h/2$ and $\varepsilon = 0.9$. We see from these figures that a numerical solution converges to the non-trivial stationary solution if α is sufficiently large. Moreover, by comparing Fig. 2 (iv) with Fig. 3 (iv), we observe that the shape of a nontrivial stationary solution depends on that of an initial function. On the other hand, the numerical solution decays to the trivial solution $u \equiv \alpha/(2\pi)$ if α is small.

In order to check that finite-difference solutions converge to stationary solutions, we observe

$$\delta_n = \frac{\|\mathbf{u}^n - \mathbf{u}^{n-1}\|_\infty}{\|\mathbf{u}^{n-1}\|_\infty}.$$

See Fig. 5. In each case, we observe that $\log \delta_n = -C_1 t_n + C_2$ for a sufficiently large t_n with some positive constants C_1 and C_2. This implies that δ_n decays to zero exponentially.

§ 4. Conservative finite-element method

This section is devoted to a brief review of conservative finite-element methods presented in Saito [13] and [14]. In order to avoid an unessential difficulty, we restrict our consideration to a polygonal domain Ω in $\mathbb{R}^2$. We consider a variant of the Keller-

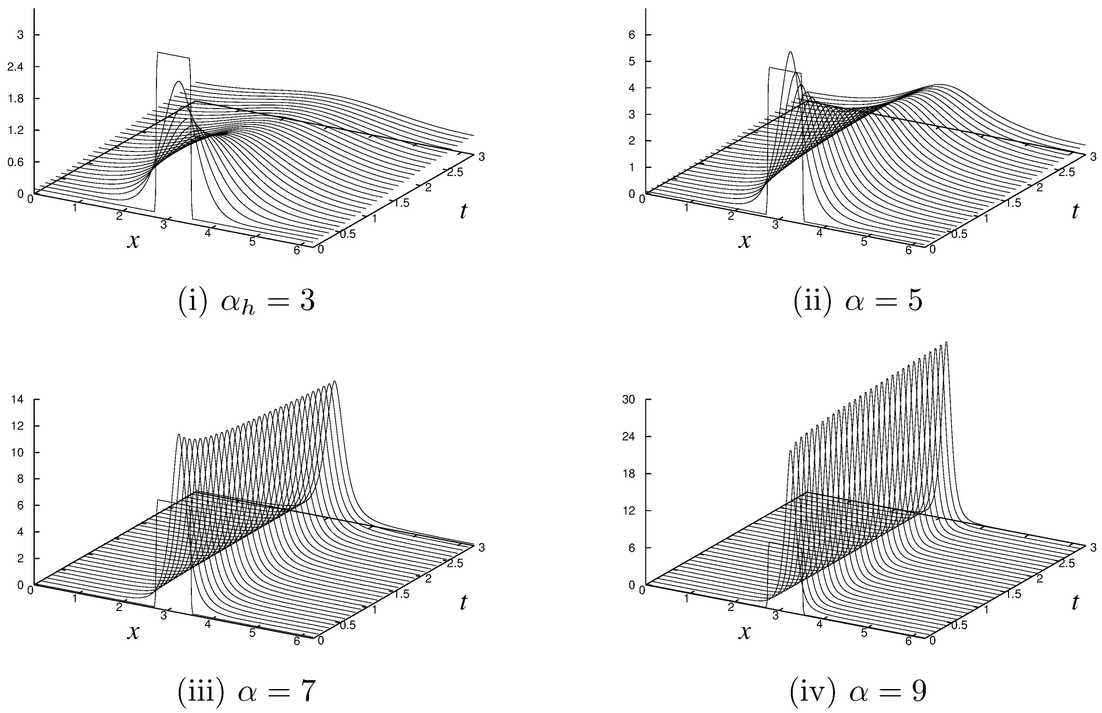

Figure 1. Behavior of the solution $\mathbf{u}^n$ of (2.3) with (3.1) and $w_1(x)$.

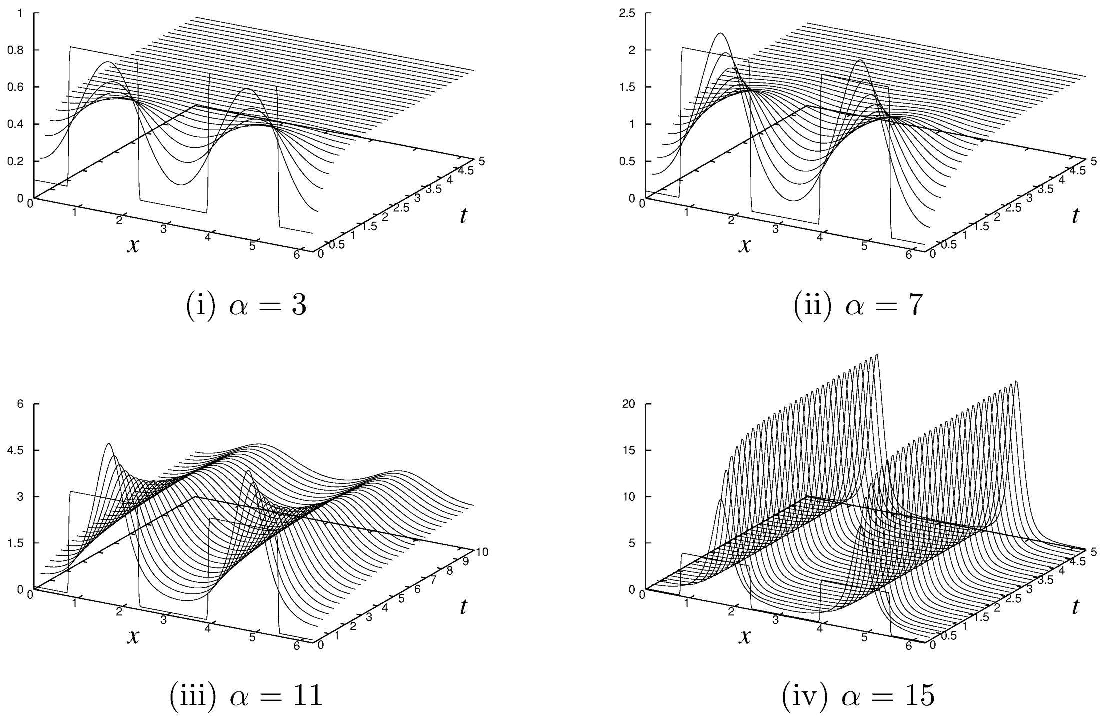

Figure 2. Behavior of the solution $\mathbf{u}^n$ of (2.3) with (3.1) and $w_2(x)$.

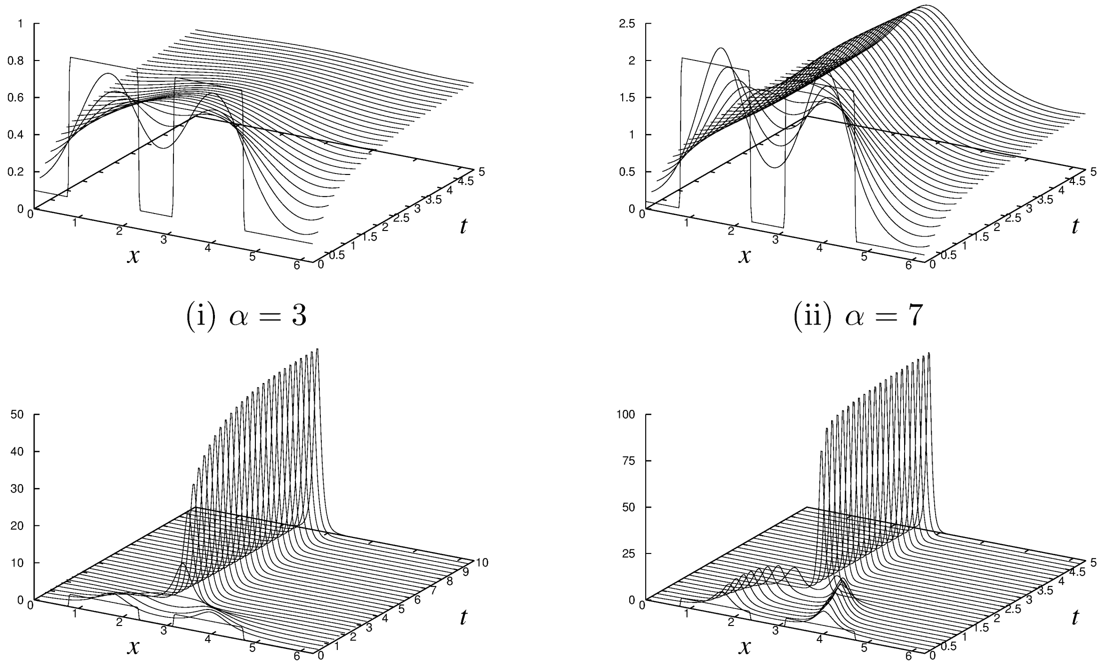

(i) $\alpha = 3$ (ii) $\alpha = 7$

(iii) $\alpha = 11$ (iv) $\alpha = 15$

Figure 3. Behavior of the solution $\mathbf{u}^n$ of (2.3) with (3.1) and $w_3(x)$.

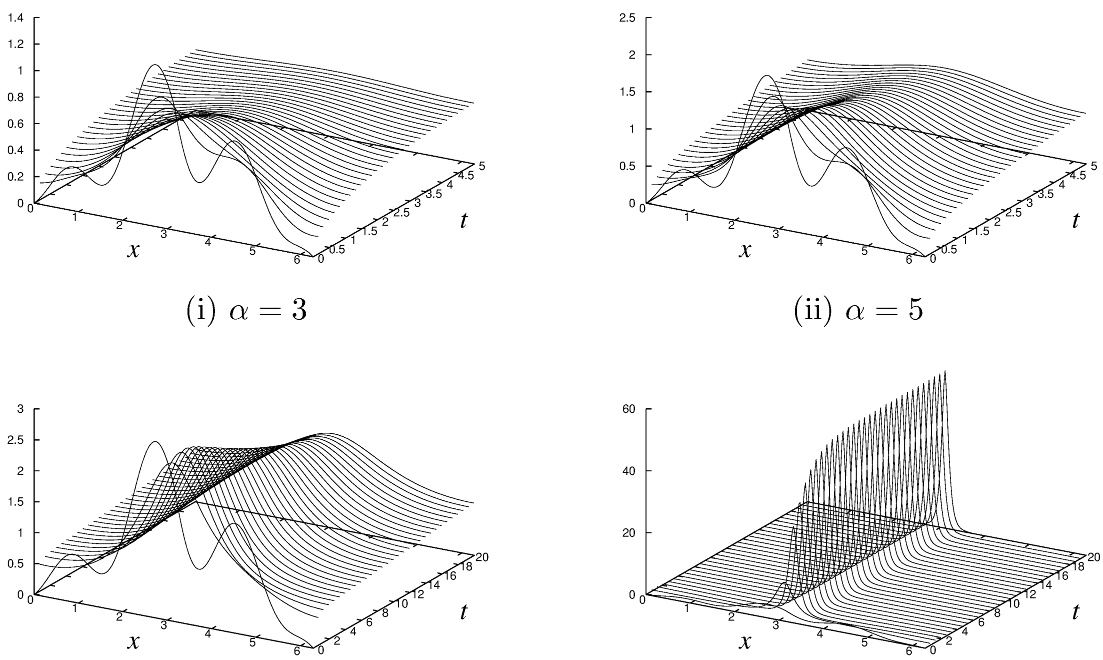

(i) $\alpha = 3$ (ii) $\alpha = 5$

(iii) $\alpha = 7$ (iv) $\alpha = 9$

Figure 4. Behavior of the solution $\mathbf{u}^n$ of (2.3) with (3.2).

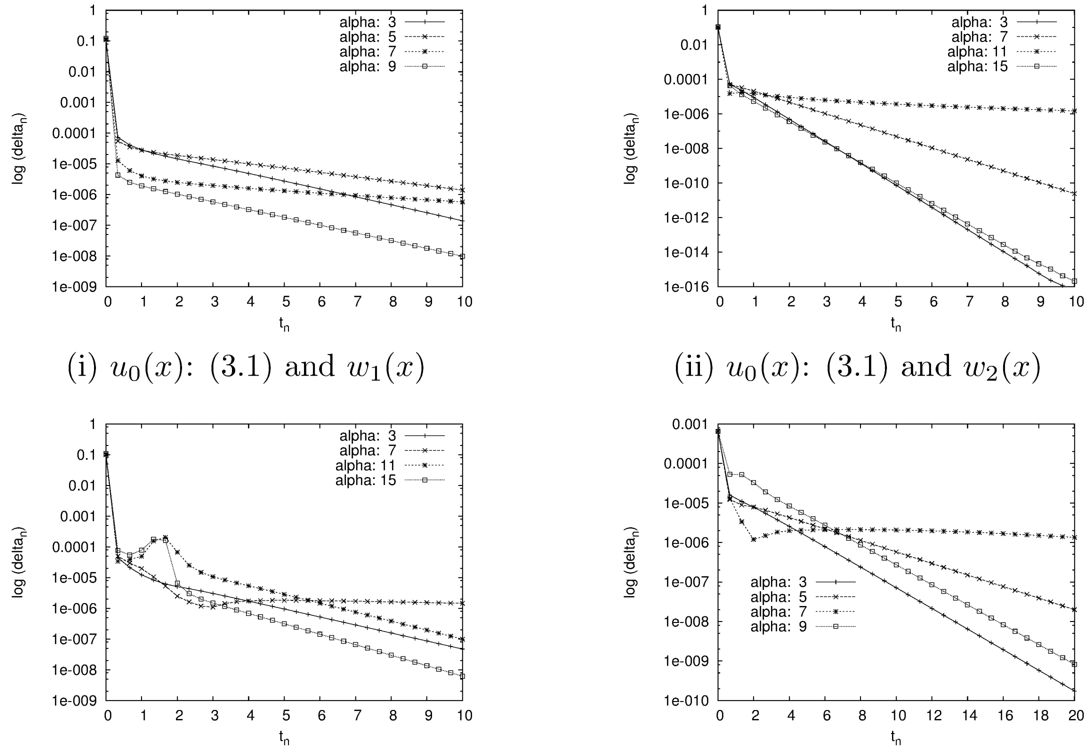

(i) $u_0(x)$: (3.1) and $w_1(x)$ (ii) $u_0(x)$: (3.1) and $w_2(x)$

(iii) $u_0(x)$: (3.1) and $w_3(x)$ (iv) $u_0(x)$: (3.2)

Figure 5. t_n vs. $\log \delta_n$.

Segel system,

$$
\text{(4.1)} \qquad \begin{cases} u_t - \nabla \cdot (D_u \nabla u - u \nabla \phi(v)) = 0 & \text{in } \Omega \times (0,T), \\ k v_t - D_v \Delta v + k_1 v - k_2 u = 0 & \text{in } \Omega \times (0,T), \\ \partial u/\partial \nu = 0,\ \partial v/\partial \nu = 0 & \text{on } \partial\Omega \times (0,T), \\ u|_{t=0} = u_0 & \text{on } \Omega, \\ v|_{t=0} = v_0 & \text{on } \Omega. \end{cases}
$$

Here, $u = u(x,t)$ and $v = v(x,t)$ are unknown functions defined in $\overline{\Omega} \times [0,T]$ to be solved; ν is the outer unit normal vector to $\partial\Omega$ and $\partial/\partial\nu$ is the differentiation along ν; D_u, D_v, k, k_1, k_2, T are positive constants; $\phi : [0,\infty) \to \mathbb{R}$ denotes a smooth function; $u_0(x), v_0(x)$ are initial functions which are assumed to be non-negative and not to be identically zero. We also consider a simplified version of Keller-Segel system,

$$
\text{(4.2)} \qquad \begin{cases} u_t - \nabla \cdot (D_u \nabla u - \lambda u \nabla v) = 0 & \text{in } \Omega \times (0,T), \\ -D_v \Delta v + k_1 v - k_2 u = 0 & \text{in } \Omega \times (0,T), \\ \partial u/\partial \nu = 0,\ \partial v/\partial \nu = 0 & \text{on } \partial\Omega \times (0,T), \\ u|_{t=0} = u_0 & \text{on } \Omega, \end{cases}
$$

where λ is a positive constant.

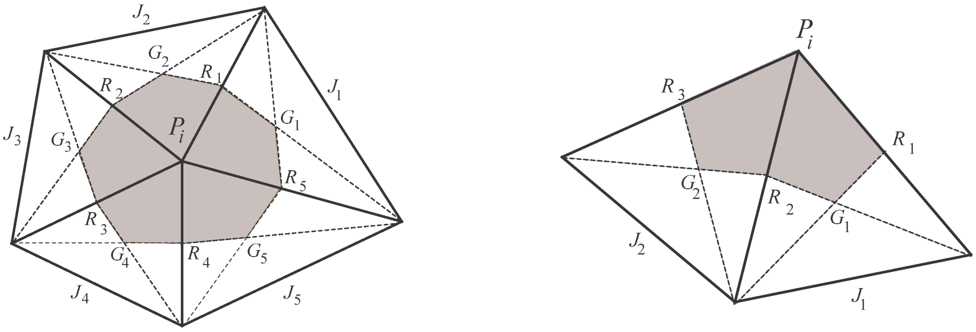

(i) P_i: interior node (ii) P_i: boundary node

Figure 6. The shaded region represents the barycentoric domain D_i corresponding to a node P_i. (G_l is the barycentor of an element J_l, and R_j is the midpoint of an edge.)

Below, we use the standard Sobolev spaces (cf. [1]). We set $W^{m,p} = W^{m,p}(\Omega)$, $H^m = W^{m,2}$, $L^p = L^p(\Omega)$, $\|\cdot\|_{m,p} = \|\cdot\|_{W^{m,p}}$, $\|\cdot\|_p = \|\cdot\|_{L^p}$ for $m \in \mathbb{N}$ and $p \in [1,\infty]$. The standard inner product in L^2 is denoted by $(\cdot,\cdot)$;

$$(u,v) = \int_\Omega u(x)v(x)\,dx.$$

First, we recall a weak formulation of (4.1): Find $u \in C^1([0,T] : H^1)$ and $v \in C^1([0,T] : H^1)$ such that

$$(4.3)\qquad \begin{cases} \left(\dfrac{du(t)}{dt},\chi\right) + (D_u\nabla u(t),\nabla\chi) + b(v(t),u(t),\chi) = 0 & (\chi \in H^1), \\ \left(k\dfrac{dv(t)}{dt},\chi\right) + (D_v\nabla v(t),\nabla\chi) + (k_1 v(t) - k_2 u(t),\chi) = 0 & (\chi \in H^1), \\ u(0) = u_0,\ v(0) = v_0, \end{cases}$$

where

$$b(v,u,\chi) = -\int_\Omega u\nabla\phi(v)\cdot\nabla\chi\,dx.$$

Let $\{\mathscr{T}_h\} = \{\mathscr{T}_h\}_{h\downarrow 0}$ be a regular family of triangulations $\mathscr{T}_h$ of Ω:

1. $\mathscr{T}_h$ is a set of closed triangles (elements) J, and $\overline{\Omega} = \bigcup\{J \mid J \in \mathscr{T}_h\}$;
2. any two elements of $\mathscr{T}_h$ meet only in entire common faces or sides or in vertices;
3. there exists a positive constant γ_1 such that

$$h_J \le \gamma_1\rho_J \quad \forall J \in \mathscr{T}_h \in \{\mathscr{T}_h\}_h,$$

where h_J and ρ_J stand for the diameters of the circumscribed and inscribed circles of J, respectively.

As the granularity parameter, we have employed $h = \max\{h_J | \ J \in \mathscr{T}_h\}$. Let $\{P_i\}_{i=1}^N$ be the set of all vertices of $\mathscr{T}_h$, $N = N_h$ being a positive integer. With P_i, we associate $\hat{\phi}_i \in C(\overline{\Omega})$ such that $\hat{\phi}_i$ is an affine function on each $J \in \mathscr{T}_h$ and $\hat{\phi}_i(P_j) = \delta_{ij}$, where δ_{ij} denotes Kronecker's delta. We define as

$$X_h = \text{ the vector space spanned by } \{\hat{\phi}_i\}_{i=1}^N$$

and regard it as a closed subspace of H^1. We also consider the space X_h, which is equipped with the topology induced from L^2, and express it using the same symbol X_h. The Lagrange interpolation operator corresponding to $\mathscr{T}_h$ is denoted by $\pi_h : C(\overline{\Omega}) \to X_h$;

$$\pi_h \chi = \sum_{i=1}^N \chi(P_i)\hat{\phi}_i \qquad (\chi \in C(\overline{\Omega})).$$

We introduce the barycentric domain D_i corresponding to a node P_i by examples; See Fig. 6. Let $\overline{\phi}_i \in L^\infty$ be the characteristic function of D_i. We introduce the vector space $\overline{X}_h$ spanned by $\{\overline{\phi}_i\}_{i=1}^N$. The operator $M_h : X_h \to \overline{X}_h$ is defined as

$$M_h \chi_h = \sum_{i=1}^N \chi_h(P_i)\overline{\phi}_i \qquad (\chi_h \in X_h),$$

which is called the lumping operator. We put

$$(v_h, \chi_h)_h = (M_h v_h, M_h \chi_h) \qquad (v_h, \chi_h \in X_h).$$

Thereby, $(\cdot,\cdot)_h^{1/2}$ is equivalent to $\|\cdot\|_2$ on X_h.

As an approximation of the trilinear form $b(v, u, \chi)$, we take

$$b_h(v, u_h, \chi_h) = \sum_{i=1}^N \chi_h(P_i) \sum_{j \in \Lambda_i} \left\{u_h(P_i)\beta_{ij}^+(v) - u_h(P_j)\beta_{ij}^-(v)\right\}$$
$$(v \in C(\overline{\Omega}),\ u_h, \chi_h \in X_h),$$

where

$$\begin{aligned}
\Lambda_i &= \{P_j \mid P_i \text{ and } P_j \text{ share an edge}\};\\
\beta_{ij}^{\pm}(v) &= \int_{\Gamma_{ij}} [\nabla \pi_h \phi(v) \cdot \nu_{ij}]_{\pm} \ dS \quad ([a]_\pm = \max\{0, \pm a\});\\
\Gamma_{ij} &= \partial D_i \cap \partial D_j;\\
\nu_{ij} &= \text{ the outer unit normal vector to } \Gamma_{ij} \text{ with respect to } D_i.
\end{aligned}$$

We note that, since $\nabla \pi_h \phi(v)$ is a constant vector in each J, $\beta_{ij}^\pm(v)$ can be expressed as

$$\beta_{ij}^\pm(v) = \sum_{J \in S_h^{ij}} \mathrm{meas}\,(\Gamma_{ij}^J) \cdot \left[(\nabla \pi_h \phi(v))|_J \cdot \nu_{ij}^J \right]_\pm ,$$

where $S_h^{i,j} = \{J \in \mathscr{T}_h |\ P_i, P_j \in J\}$; meas (Γ_{ij}^J) is the length of Γ_{ij}^J, and Γ_{ij}^J; ν_{ij}^J are restrictions of Γ_{ij}, ν_{ij} to J, respectively.

Although this is a direct application of Baba and Tabata's scheme (cf. [2]), we briefly state its derivation in a formal manner:

$$\begin{aligned}
b(v,u,\chi) &= \int_\Omega \nabla\left(u\nabla\phi(v)\right)\chi_h\ dx && \text{(integration by parts)}\\
&\approx \sum_{i=1}^N \chi_h(P_i)\int_{D_i}\nabla\left(u_h\nabla\phi(v)\right)\ dx && (\chi\approx\chi_h\approx M_h\chi_h)\\
&= \sum_{i=1}^N \chi_h(P_i)\sum_{j\in\Lambda_i}\int_{\Gamma_{ij}} u\nabla\phi(v)\cdot\nu_{ij}\ dS && \text{(divergence theorem)}\\
&\approx \sum_{i=1}^N \chi_h(P_i)\sum_{j\in\Lambda_i}\int_{\Gamma_{ij}} u_h\nabla\pi_h\phi(v)\cdot\nu_{ij}\ dS && (\phi(v)\approx\pi_h\phi(v))\\
&\approx \sum_{i=1}^N \chi_h(P_i)\sum_{j\in\Lambda_i}\int_{\Gamma_{ij}} \overline{u}_h\nabla\pi_h\phi(v)\cdot\nu_{ij}\ dS && (u\approx u_h\approx\overline{u}_h\equiv M_h u_h).
\end{aligned}$$

The last integral, however, does not make a sense, since the value of $\overline{u}_h$ is not defined on Γ_{ij}. Then, the last integral is approximated by considering the upwind nodal points as follows:

$$\begin{aligned}
\int_{\Gamma_{ij}} \overline{u}_h\nabla\pi_h\phi(v)\cdot\nu_{ij}\ dS &= \int_{\Gamma_{ij}} \overline{u}_h[\nabla\pi_h\phi(v)\cdot\nu_{ij}]_+ dS - \int_{\Gamma_{ij}} \overline{u}_h[\nabla\pi_h\phi(v)\cdot\nu_{ij}]_- dS\\
&\approx u_h(P_i)\beta_{ij}^+(v) - u_h(P_j)\beta_{ij}^-(v)
\end{aligned}$$

Thus, we obtain $b_h(v,u_h,\chi_h)$ as an approximation $b(v,u,\chi)$.

The time variable is discretized as

$$t_n = \tau_1+\tau_2+\cdots+\tau_n, \qquad \tau_n > 0.$$

Then, we consider the finite-element scheme to obtain an approximation (u_h^n, v_h^n) of the solution $(u(t_n), v(t_n))$ of (4.1): Find $\{u_h^n\}_{n\geq 0}\subset X_h$ and $\{v_h^n\}_{n\geq 0}\subset X_h$ such that

$$\text{(4.4)}\qquad \begin{cases}
\left(\dfrac{u_h^n - u_h^{n-1}}{\tau_n}, \chi_h\right)_h + (D_u\nabla u_h^n, \nabla\chi_h) + b_h(v_h^{n-1}, u_h^n, \chi_h) = 0\\[2ex]
\left(k\dfrac{v_h^n - v_h^{n-1}}{\tau_n}, \chi_h\right)_h + (D_v\nabla v_h^n, \nabla\chi_h) + (k_1 v_h^n - k_2 u_h^n, \chi_h)_h = 0\\
\hfill (\chi_h\in X_h,\ n\geq 1),\\[1ex]
u_h^0 = u_{0h},\ v_h^0 = v_{0h}.
\end{cases}$$

Here u_{0h} and v_{0h} denote suitable approximations of u_0 and v_0. A typical choice is $u_{0h} = \pi_h u_0$ and $v_{0h} = \pi_h v_0$. The first and second equations of (4.4) are linear systems for u_h^n and v_h^n. In fact, substituting $\chi_h = \hat{\phi}_i$ into (4.4), we have

$$\frac{u_h^n(P_i) - u_h^{n-1}(P_i)}{\tau_n} m_i + \sum_{j=1}^{N} \{D_u a_{ij} + b_{ij}(v_h^{n-1})\} u_h^n(P_j) = 0,$$

$$k\frac{v_h^n(P_i) - v_h^{n-1}(P_i)}{\tau_n} m_i + \sum_{j=1}^{N} D_v a_{ij} + (k_1 v_h^n(P_i) - k_2 u_h^n(P_i))\, m_i = 0,$$

where

$$m_i = \text{ the area of } D_i; \quad a_{ij} = (\nabla\hat{\phi}_j, \nabla\hat{\phi}_i); \quad b_{ij}(w) = b_h(w, \hat{\phi}_j, \hat{\phi}_i).$$

Thus, if we set

$$\mathsf{u}^n = (u_h^n(P_1), \dots, u_h^n(P_N))^{\mathrm{T}}, \quad \mathsf{v}^n = (v_h^n(P_1), \dots, v_h^n(P_N))^{\mathrm{T}},$$
$$\mathsf{A} = [a_{ij}], \quad \mathsf{B}^n = [b_{ij}(v_h^n)], \quad \mathsf{M} = \mathrm{diag}\,[m_1, \dots, m_N],$$

then (4.4) is expressed as

$$\left[\mathsf{M} + \tau_n D_u \mathsf{A} + \tau_n \mathsf{B}^{n-1}\right] \mathsf{u}^n = \mathsf{M}\mathsf{u}^{n-1},$$
$$\left[\left(1 + \frac{\tau_n k_1}{k}\right)\mathsf{M} + \frac{\tau_n}{k} D_v \mathsf{A}\right] \mathsf{v}^n = \mathsf{M}\mathsf{v}^{n-1} + \frac{\tau_n k_2}{k}\mathsf{M}\mathsf{u}^n.$$

We recall that $a_{ij} = b_{ij}(w) = 0$ when P_i and P_j share no edge.

On the other hand, our finite-element scheme to (4.2) is as follows: Find $\{u_h^n\}_{n\geq 0} \subset X_h$ and $\{v_h^n\}_{n\geq 0} \subset X_h$ such that

$$(4.5) \qquad \begin{cases} \left(\dfrac{u_h^n - u_h^{n-1}}{\tau_n}, \chi_h\right)_h + (D_u \nabla u_h^n, \nabla\chi_h) + b_h(v_h^{n-1}, u_h^n, \chi_h) = 0 \\ (D_v \nabla v_h^{n-1}, \nabla\chi_h) + (k_1 v_h^{n-1} - k_2 u_h^{n-1}, \chi_h)_h = 0 \qquad (\chi_h \in X_h,\ n \geq 1), \\ u_h^0 = u_{0h}, \end{cases}$$

where we have set $\phi(v) = \lambda v$.

Remark. The semi-implicit time discretization employed in (4.4) and (4.5) is closely related to the reproduction of Lyapunov's property, which is another important feature of the system (4.1) and (4.2). For further details and other methods of time discretization, we refer to Saito and Suzuki [15].

Our finite-element solutions enjoy fine conservative properties. Below we recall only the statement of theorems and we refer to Saito [13] and [14] for the complete proof. The first one is related to the discrete version of the conservation of total mass.

Theorem 4.1 (Conservation of total mass). *Let* $\{(u_h^n, v_h^n)\}_{n\geq 0} \subset X_h$ *be a solution of (4.4) or (4.5). Then, we have* $(u_h^n, 1)_h = (u_{0h}, 1)_h$ *for* $n \geq 0$.

The second one is related to the well-posedness of our schemes including the discrete version of conservation of positivity. To state it, we set

$$\kappa_h = \min_{J\in\mathscr{T}_h} \kappa_J \qquad (\kappa_J = \text{ the minimal perpendicular length of } J)\,.$$

Theorem 4.2 (Well-posedness and conservation of positivity). *Suppose that* $\{\mathscr{T}_h\}$ *is of acute type, i.e., each* $J \in \mathscr{T}_h$ *is an acute or a right triangle. Assume that* $u_{0h}, v_{0h} \in X_h$ *are non-negative and is not identically constant. Take* $\tau > 0$ *and* $\varepsilon \in (0, 1]$. *Then, (4.4) or (4.5) with a time step-size control*

$$\tau_n = \min\left\{\tau, \quad \frac{\varepsilon\kappa_h}{4\|\nabla\pi_h\phi(v_h^{n-1})\|_\infty}\right\}$$

admits a unique solution $\{(u_h^n, v_h^n)\}_{n\geq 0} \subset X_h$ *such that* $u_h^n > 0$ *for* $n \geq 1$.

Combining this with Theorem 4.1, we immediately obtain

Theorem 4.3 (Conservation of the L^1 norm). *Let* $\{(u_h^n, v_h^n)\}_{n\geq 0} \subset X_h$ *be a solution of (4.4) or (4.5) as in Theorem 4.2. Then, we have* $\|u_h^n\|_1 = \|u_{0h}\|_1$ *for* $n \geq 0$.

Remark. There is a constant $c_h > 0$ such that $\tau_n \geq \min\{\tau, c_h\}$. Thus, τ_n never converges to zero as n increases, and therefore the algorithm always works. Consequently, u_h^n actually exists for all $n \geq 1$.

To state a convergence result, we make the following condition:

(R) *Elliptic regularity.* There exists $\mu \in (2, \infty)$ such that the following holds true: For any $p \in (1, \mu)$ and $f \in L^p(\Omega)$, the linear elliptic problem

$$-\Delta v + v = f \quad \text{in } \Omega, \quad \frac{\partial v}{\partial \nu} = 0 \quad \text{on } \partial\Omega$$

admits a unique solution $v \in W^{2,p}$ that satisfies

$$\|v\|_{2,p} \leq C\|f\|_p$$

with a constant $C = C(p, \Omega) > 0$.

Remark. When Ω is a convex polygon, (R) is satisfied (cf. Grisvard [5]).

For the sake of simplicity, we consider only (4.2) and (4.5).

Theorem 4.4 (Error estimates). *Suppose that $\{\mathscr{T}_h\}$ is of acute type and of inverse property; there exists a positive constant γ_2 such that*

$$\gamma_2 h \le h_J \quad \forall J \in \mathscr{T}_h \in \{\mathscr{T}_h\}.$$

Assume that (4.2) admits a unique solution (u, v) satisfying

$$u \in C([0,T] : W^{2,p}), \quad u_t \in C([0,T] : W^{1,p}) \cap C^\sigma([0,T] : L^p) \tag{4.6}$$

for some $p \ge 2$, $\sigma \in (0,1]$. Moreover, let $u_{0h} \in X_h$ be chosen as

$$\|u_0 - u_{0h}\|_p \le \alpha_{0,p} h^{1-2/p},$$

with a constant $\alpha_{0,p} = \alpha_{0,p}(u_0) > 0$. Then, there exist positive constants h_0, τ_0 and C_0 independent of h and τ such that we have the error estimate

$$\sup_{0 \le t_n \le T} (\|u(t_n) - u_h^n\|_p + \|v(t_n) - v_h^n\|_{1,\infty}) \le C_0(h^{1-2/p} + \tau^\sigma) \tag{4.7}$$

for $h \in (0, h_0)$ and $\tau \in (0, \tau_0)$, where $\{(u_h^n, v_h^n)\}_{n \ge 0} \subset X_h$ is the solution of (4.5) as in Theorem 4.2.

Remark. Under the regularity assumption (4.6), we set

$$\alpha_{1,p} = \sup_{t \in [0,T]} \|u(t)\|_{2,p}, \quad \alpha_{2,p} = \sup_{t \in [0,T]} \|u_t(t)\|_{1,p}\,, \quad \alpha_{3,p} = \sup_{t,s \in [0,T]} \frac{\|u_t(t) - u_t(s)\|_p}{|t-s|^\sigma}.$$

Then, the constant C_0 in (4.7) can be taken as

$$C_0 = C(T+1)(\alpha_{0,p} + \alpha_{1,p}^2 + \alpha_{2,p}^2 + \alpha_{3,p}) \exp\left[C'(1 + \alpha_{1,p}^2)T\right],$$

where C and C' are positive constants that depend only on Ω, k, λ, γ_i's, h_0 and τ_0.

Remark. If we consider a bounded domain $\Omega \subset \mathbb{R}^2$ with the sufficiently smooth boundary $\partial\Omega$ and take a regular family of (curved) triangulations $\{\mathscr{T}_h\}_h$, which *exactly fit the boundary*:

$$\overline{\Omega} = \bigcup_{J \in \mathscr{T}_h} J.$$

Then, we can refine (4.7) and obtain

$$\sup_{0 \le t_n \le T} (\|u(t_n) - u_h^n\|_p + \|v(t_n) - v_h^n\|_{1,\infty}) \le C_0'(h + \tau^\sigma).$$

Remark. Concerning (4.1) and (4.4), we have a convergence result of the form (4.7); we refer to Saito [14].

§ 5. Numerical results (2D case)

In this section, we report some results of numerical experiments by conservative finite-element schemes (4.4) and (4.5).

We assume that $\Omega \subset \mathbb{R}^2$ is a unit square: $\Omega = (0,1)^2$. We take $\mathscr{T}_h$ as a uniform mesh composed of $2\ell^2$ congruent right-angle triangles for $\ell \in \mathbb{N}$; each side of Ω is divided into ℓ intervals of the same length. Then each small square is decomposed into two equal triangles by a diagonal. Then we have $h = \sqrt{2}\ell^{-1}$. Further, we set $\alpha = \|u_{0h}\|_1$.

First, we consider the simplified system (4.2) and its finite-element approximation (4.5), where $\phi(v) = \lambda v$, $D_u = D_v = 1$ and $\lambda = k_1 = k_2 = 1$. Fig. 7 shows the behavior of the solution u_h^n of (4.5) with $\alpha = 6.2$: (i) the initial function has one peak and it is located near a corner; (ii) it moves to the corner; (iii, iv) it is smoothed and becomes a flat surface. On the other hand, the result when $\alpha = 7.6$ is illustrated in Fig. 8 where a larger and sharper peak is produced at the corner. We compare the magnitude of those two solutions in Fig. 9 where the shapes of $\log(1 + u_h^n)$ are displayed.

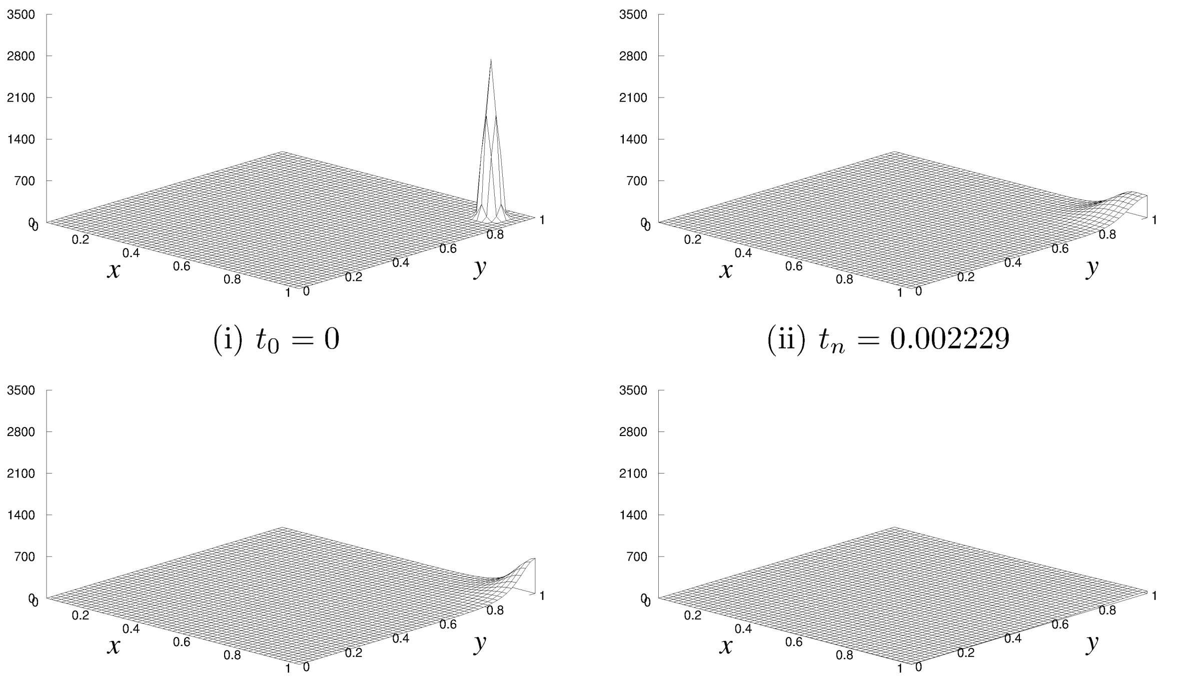

(i) $t_0 = 0$ (ii) $t_n = 0.002229$

(iii) $t_n = 0.016673$ (iv) $t_n = 0.333343$

Figure 7. Behavior of the solution u_h^n of (4.5) with $\alpha = 6.2$. ($\ell = 100$; $\tau = h/2$; $\varepsilon = 0.9$; $D_u = D_v = \lambda = k_1 = k_2 = 1$; $\phi(v) = v$)

According to Gajewski and Zacharias [4], if $\|u_0\|_1 \le 2\pi$ and $\Omega = (0,1)^2$, the full system (4.1) admits a unique time-global solution such that $\|u(t)\|_\infty \le c(t)$, where $t \mapsto c(t)$ denotes a nondecreasing finite function. Our result, Fig. 7, supports that this

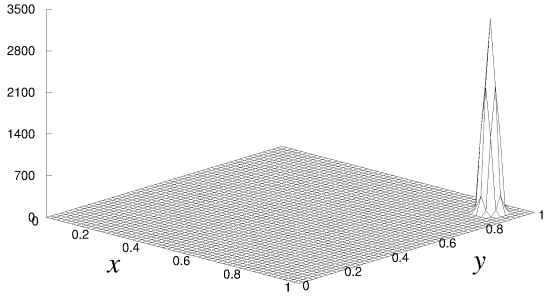

(i) $t_0 = 0$

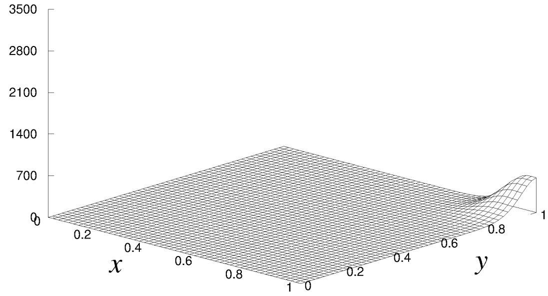

(ii) $t_n = 0.003335$

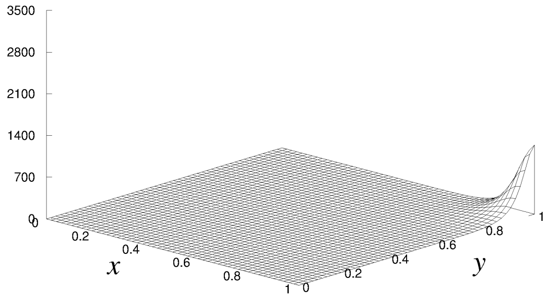

(iii) $t_n = 0.006667$

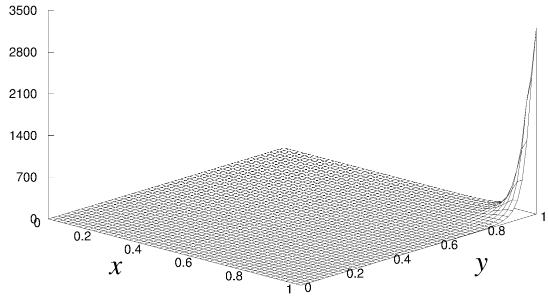

(iv) $t_n = 1.000003$

Figure 8. Behavior of the solution u_h^n of $\alpha = 7.6$. ($\ell = 100$; $\tau = h/2$; $\varepsilon = 0.9$; $D_u = D_v = \lambda = k_1 = k_2 = 1$; $\phi(v) = v$)

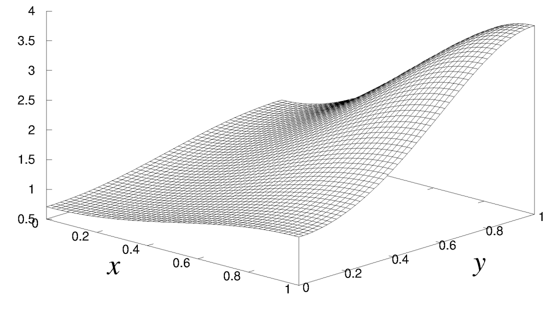

(i) $\alpha = 6.2$;
$t_n = 0.333343$

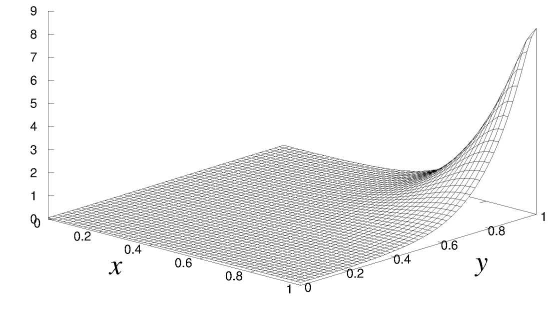

(ii) $\alpha = 7.6$;
$t_n = 1.000003$

Figure 9. Shape of $\log(1 + u_h^n)$, where u_h^n is the solution of (4.5). ($\ell = 100$; $\tau = h/2$; $\varepsilon = 0.9$; $D_u = D_v = \lambda = k_1 = k_2 = 1$; $\phi(v) = v$)

analytical result is still valid for the the simplified system.

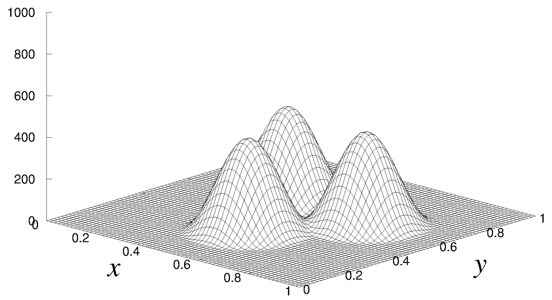

(i) $t_0 = 0$

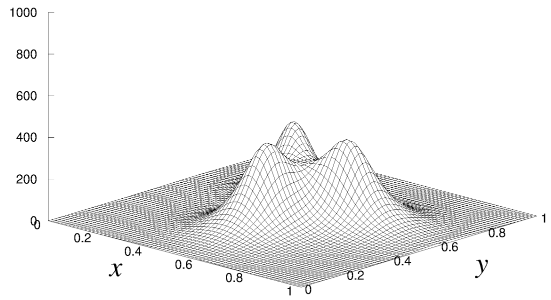

(ii) $t_n = 0.006457$

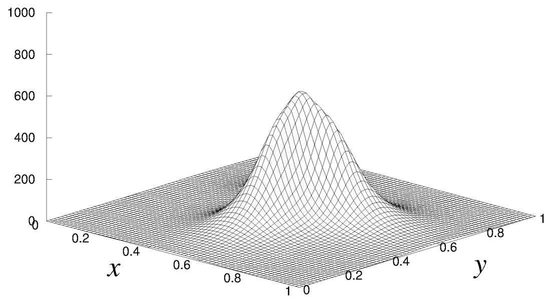

(iii) $t_n = 0.008364$

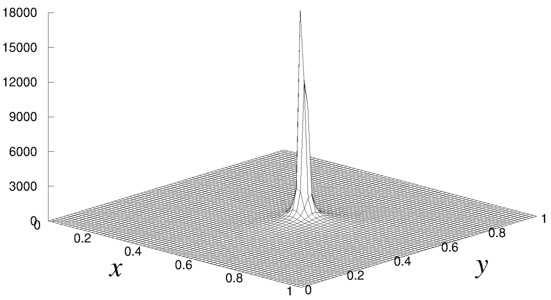

(iv) $t_n = 0.011000$

Figure 10. Behavior of the solution u_h^n of (4.4) with $k = 0.1$ ($\phi(v) = 5v^2$; $D_u = D_v = 1$, $k_1 = 0.1$; $k_2 = 0.01$; $\ell = 128$; $\tau = h/2$; $\varepsilon = 0.9$; $\alpha = 50$)

Finally, we consider the full system (4.1) and its finite element approximation (4.4), where $\phi(v) = 5v^2$, $D_u = D_v = 1$, $k_1 = 0.1$ and $k_2 = 0.01$. Fig. 10 shows the behavior of the solution u_h^n of (4.4) with $\|u_{0h}\|_1 = 50$ and $k = 0.1$: (i) the initial function has three peaks; (ii, iii, iv) they gather and produce a single peak. On the other hand, Fig. 11 shows the behavior of u_h^n with the same initial function and another value of k ($k = 0.001$). In this case, each peak becomes higher and shaper individually. Especially, they do not gather. The difference of the relaxation time k causes such an interesting phenomena.

§ 6. Concluding remarks

We have reviewed conservative finite-difference and finite-element methods applied to the Keller-Segel systems and reported some new numerical results. In §3, we considered a simplified Keller-Segel system in a unit circle and gave some numerical results which show that the solution converges to the non-trivial stationary solution if $\|u_{0h}\|_1$ is sufficiently large. Moreover, we observed that the shape of a nontrivial stationary solution depends on that of an initial function, and the solution decays to the trivial

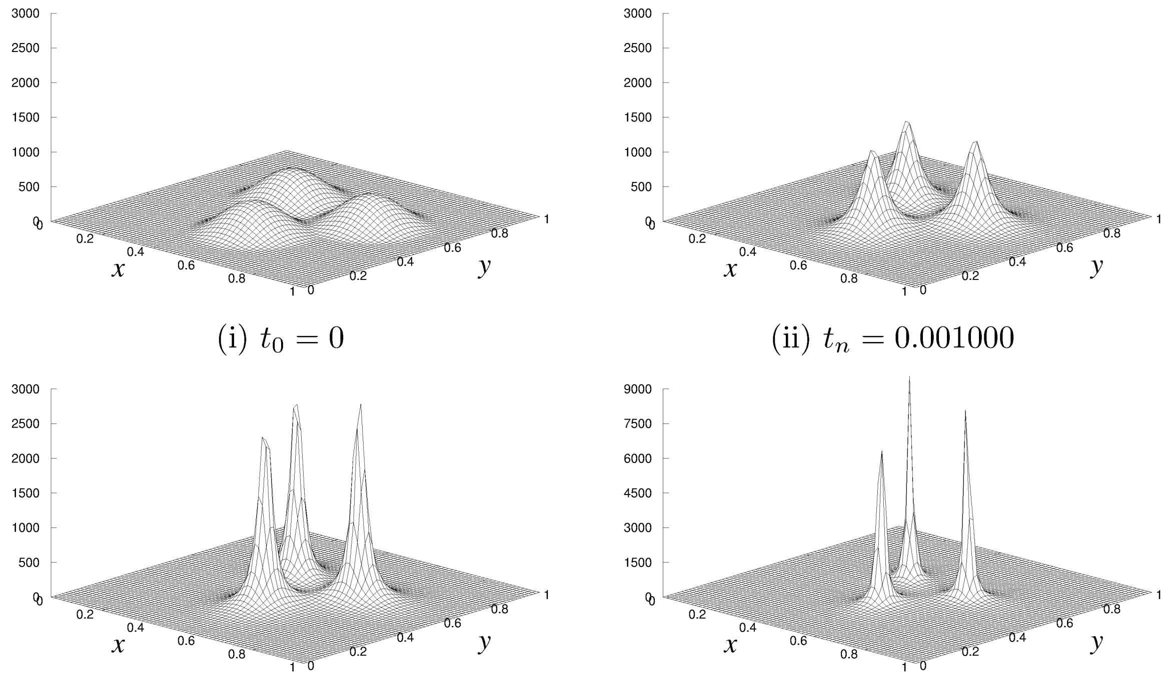

(i) $t_0 = 0$ (ii) $t_n = 0.001000$

(iii) $t_n = 0.001347$ (iv) $t_n = 0.001613$

Figure 11. Behavior of the solution u_h^n of (4.4) with $k = 0.001$ ($\phi(v) = 5v^2$; $D_u = D_v = 1$, $k_1 = 0.1$; $k_2 = 0.01$; $\ell = 128$; $\tau = h/2$; $\varepsilon = 0.9$; $\|u_{0h}\|_1 = 50$)

solution if $\|u_{0h}\|_1$ is small. Furthermore, in §5, we gave some numerical examples for 2D cases and showed that highly concentrated solutions are captured successfully. Our numerical results support analytical results of Gajewski and Zacharias [4] concerning global and bounded solutions. Thus, while the solution remains bounded if $\|u_{0h}\|_1$ is small, the solution produce a larger and sharper peak if $\|u_{0h}\|_1$ is large. However, we cannot see that whether the solution blows up in finite time. Indeed, our finite-element solution never blows up in finite time, since its L^1 norm is exactly preserved. With this connection, we consider the same situation as Fig. 7 and plot in Fig. 12 the value of $\log \|u_h^n\|_\infty$ for $\alpha \equiv \|u_{0h}\|_1 = 6.2, 6.4, \ldots, 8.0$. We observe from those figures that a numerical solution grows faster than exponential functions in a short time interval $[0, t^*]$. The behavior after that ($t > t^*$) depends on cases. When $\ell = 60$, every solution decays exponentially. On the other hand, when $\ell = 120$, solutions corresponding to $6.2 \le \alpha \le 7.4$ decay exponentially and other solutions grow exponentially. We infer from this observation that the fixed space mesh is inadequate to capture the blow up phenomenon and application of some new devices, for example, adaptive mesh refinement based on a posteriori analysis, is required. They are left here as future study.

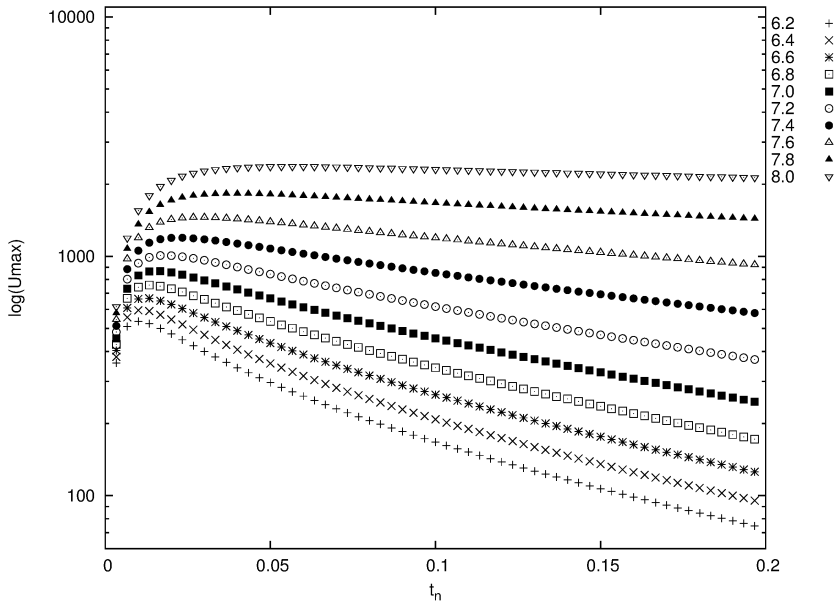

(i) $\ell = 60$

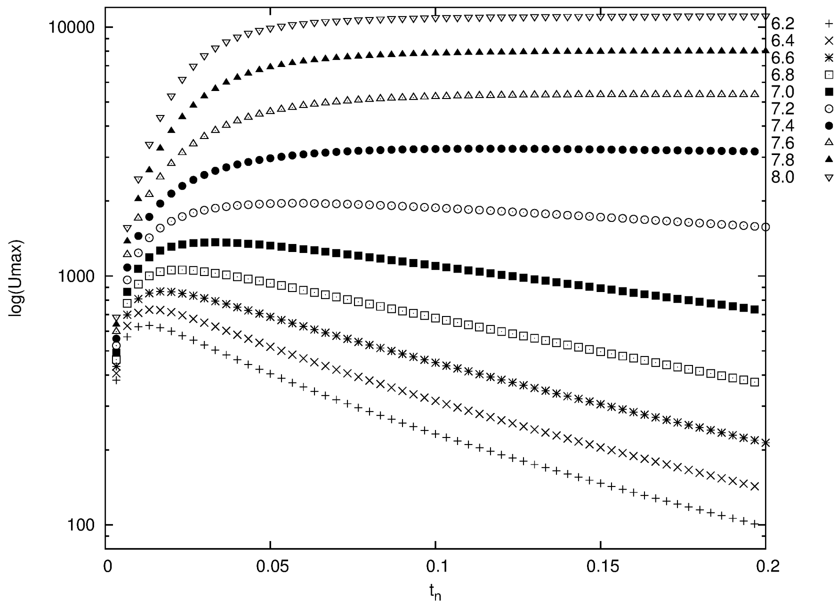

(ii) $\ell = 120$

Figure 12. t_n vs. $\log \|u_h^n\|_\infty$ for several values of α. ($\tau = h/2$; $\varepsilon = 0.9$; $D_u = D_v = \lambda = k_1 = k_2 = 1$; $\phi(v) = v$)

References

[1] R. A. Adams and J. Fournier, *Sobolev Spaces*, Second Edition, Academic Press, 2003.

[2] K. Baba and T. Tabata, *On a conservative upwind finite-element scheme for convective diffusion equations*, RAIRO Anal. Numér., **15** (1981), 3–25.

[3] F. Filbet, *A finite volume scheme for Patlak-Keller-Segel chemotaxis model*, Numer. Math., **104** (2006), 457–488.

[4] H. Gajewski and K. Zacharias, *Global behaviour of a reaction-diffusion system modelling chemotaxis*, Math. Nachr., **195** (1998), 77–114.

[5] P. Grisvard, *Elliptic Problems in Nonsmooth Domains*, Pitman, 1985.

[6] D. Horstmann, *From 1970 until present: the Keller-Segel model in chemotaxis and its consequences I*, Jahresber. Deutsch. Math.-Verein., **105** (2003), 103–165.

[7] D. Horstmann, *From 1970 until present: the Keller-Segel model in chemotaxis and its consequences II*, Jahresber. Deutsch. Math.-Verein., **106** (2004), 51–89.

[8] F. F. Keller and L. A. Segel, *Initiation on slime mold aggregation viewed as instability*, J. Theor. Biol., **26** (1970), 399–415.

[9] A. Kubo, N. Saito, T. Suzuki and H. Hoshino, *Mathematical models of tumor angiogenesis and simulations*, Kôkyûroku, Research Institute for Mathematical Sciences, Kyoto University, **1499** (2006), 135–146.

[10] A. Marrocco, *Numerical simulation of chemotactic bacteria aggregation via mixed finite-elements*, M2AN Math. Model. Numer. Anal., **37** (2003) 617–630.

[11] E. Nakaguchi and Y. Yagi, *Fully discrete approximation by Galerkin Runge-Kutta methods for quasilinear parabolic systems*, Hokkaido Math. J., **31** (2002), 385–429.

[12] T. Ooura, *Ooura's Mathematical Software Packages*, http://www.kurims.kyoto-u.ac.jp/˜ooura/index.html

[13] N. Saito, *Conservative upwind finite-element method for a simplified Keller-Segel system modelling chemotaxis*, IMA J. of Numer. Anal., **27** (2007), 332–365.

[14] N. Saito, *Error analysis of conservative upwind finite-element approximation for the Keller-Segel system of chemotaxis*, in preparation.

[15] N. Saito and T. Suzuki, *Notes on finite difference schemes to a parabolic-elliptic system modelling chemotaxis*, Appl. Math. Comput., **171** (2005), 72–90.

[16] T. Suzuki, *Free Energy and Self-Interacting Particles*, Birkhauser, 2005.